

N 7 2 - 2 5 4 9 2

NATIONAL AERONAUTICS AND SPACE ADMINISTRATION

Technical Report 32-1557

*Initiation of Insensitive Explosives
by Laser Energy*

Vincent J. Menichelli

Lein C. Yang

**CASE FILE
COPY**

**JET PROPULSION LABORATORY
CALIFORNIA INSTITUTE OF TECHNOLOGY
PASADENA, CALIFORNIA**

June 1, 1972

NATIONAL AERONAUTICS AND SPACE ADMINISTRATION

Technical Report 32-1557

*Initiation of Insensitive Explosives
by Laser Energy*

Vincent J. Menichelli

Lein C. Yang

**JET PROPULSION LABORATORY
CALIFORNIA INSTITUTE OF TECHNOLOGY
PASADENA, CALIFORNIA**

June 1, 1972

Preface

The work described in this report was performed by the Propulsion Division of the Jet Propulsion Laboratory.

Acknowledgment

The authors wish to acknowledge Mr. H. Jeffries for his careful fabrication of the test samples and his assistance throughout the program.

Contents

I. Introduction	1
II. Laser-Generated Shocks	2
III. Test Apparatus	2
IV. Test Results	8
V. Discussion	9
References	16

Tables

1. Conditions and results for laser testing of HNS and Dipam	8
2. Conditions and results for laser testing of PETN	9
3. Conditions and results for laser testing of RDX	10
4. Conditions and results for laser testing of tetryl	12
5. Conditions and results for selected-detonated items	12

Figures

1. Test vehicle for laser initiation study	3
2. Streak camera records of the plasma generated in a vacuum from a focused Q-switched ruby laser	3
3. Post-irradiation damage to thin aluminum films by a focused Q-switched ruby laser	4
4. Streak camera records of the plasma generated in a vacuum, for various thicknesses of aluminum films, from a focused Q-switched ruby laser	4
5. Block diagram of experimental configuration	5
6. Laboratory arrangement of laser, camera, and firing chamber	5
7. Test vehicle with plastic viewing window for laser initiation study	6
8. Test vehicle with glass tube configuration for viewing of laser initiation	7
9. Streak camera records of laser-initiated detonation in PETN (values given refer to Table 5)	13

Contents (contd)

Figures (contd)

10. Streak camera records of laser-initiated detonation in PETN
and RDX (values given refer to Table 5) 14
11. Streak camera records of laser-initiated detonation in RDX
and tetryl (values given refer to Table 5) 15

Abstract

Instantaneous longitudinal detonations have been observed in confined columns of pentaerythritol tetranitrate (PETN), cyclotrimethylene trinitramine (RDX), and tetryl when these materials were pulsed with light energy from a focused Q-switch ruby laser. The laser energy ranged from 0.5 to 4.2 J with a pulse width of 25 ns. Enhancement of the ignition mechanism is hypothesized when a 100-nm (1000-Å) thick aluminum film is vacuum-deposited on the explosive side of the window. Upon irradiation from the laser, a shock is generated at the aluminum-explosive interface. Steady-state detonations can be reached in less than 0.5 μ s with less than 10% variation in detonation velocity for PETN and RDX.

Initiation of Insensitive Explosives by Laser Energy

I. Introduction

Immediate detonation of secondary high explosives requires a strong shock input, the threshold magnitude of the shock being dependent upon such parameters as explosive density, particle size, and confinement. Conventional means of achieving detonation in secondary high explosives is by the use of the explosive train. These trains, in general, are initiated mechanically by firing pins (stab or percussion) or electrically (hot bridgewire). The first component in the train is usually a primary high explosive sensitive to heat, friction, impact, and static electricity and also having poor simultaneity characteristics. The train then proceeds with increments of less sensitive, more energetic explosives. Eventually, in a short distance, the burning reaction develops into a detonation. These systems require very little energy to initiate (0.1 J or less) and are quite vulnerable to inadvertent initiation. To ward against accidental initiation of the main charge, a Safe and Arming mechanism (S and A) is usually employed. Work has been carried out to develop insensitive explosive trains, using only secondary high explosives which will initiate from a unique energy source; e.g., strong light or exploding wire. The advantages are many fold: the elimination of primary high explosives, elimination of complicated S and As, and an improvement in simultaneity and functioning time.

Bowden et al. studied the sensitivity of explosives to strong light sources (Ref. 1), and Leopold was able to

detonate PETN with exploding bridgewires (EBW) (Ref. 2). Detonation of PETN by EBW was very dependent upon parameters such as loading density, particle size and shape, purity, bridgewire size and material, and discharge circuitry.

In order to reach immediate detonation in secondary high explosives such as PETN, RDX, and tetryl, threshold external shock strengths ranging from 7×10^5 to 15×10^5 N/m² (7 to 15 kbars) are needed (Ref. 3). In recent years, pulsed laser radiation as an energy source to initiate explosives has been studied. Space Ordnance Systems, Inc., investigated the sensitivity of pyrotechnics and propellants to laser energy under a JPL contract (Ref. 4). During this study no unconfined secondary high explosives could be initiated from a focused ruby or neodymium pulsed laser in the free-running mode (up to 15 J of energy). Barbarisi et al. at Picatinny Arsenal, New Jersey, studied the reaction of PETN to a pulsed ruby laser (focused) in the free-running and Q-switched modes (Ref. 5). Ignition was obtained in both modes but direct detonations were not confirmed. The Russians have reported similar work and successfully detonated PETN (density 1.0 g/cm³) from a pulsed ruby laser (0.5 J) in the Q-switched mode (Ref. 6). Experiments have been carried out at JPL to detonate secondary high explosives with a focused ruby laser in the Q-Switched mode (Ref. 7). Figure 1 shows a cross section of the test vehicle used. Some detonations were achieved with PETN and RDX

as witnessed from a dent obtained on a steel witness block and expansion of the steel test vehicle. The time to detonation was not known and it appeared that uncertainties such as explosive surface conditions, trapped air, impurities, and crystal imperfections were playing an important role in the initiation mechanism.

II. Laser-Generated Shocks

The interaction of Q-switched laser pulses with a solid target was known to result in rapid expanding plasmas (Ref. 8). The process, when observed with a streak camera in air at JPL was not clear, possibly due to ionization of the air by the laser. Figure 2 shows the results of experiments conducted with metal targets in a vacuum (1.33 N/m^2 , or 1 mm Hg).¹ The resulting plasma propagation is more clearly defined. An approximation of the shock is measured by the propagation of the luminous plasma boundary. From these results, application of the shock (in the order of several $\text{cm}/\mu\text{s}$) to denote secondary high explosives seemed appropriate. The mechanism is similar to EBW or exploding foil. However, the laser shock is physically different, in that the shock velocity is an order of magnitude higher and the duration shorter (a few hundred nanoseconds compared to about $2\mu\text{s}$).

Selection of target material and thickness for application to laser initiation of explosives was based on some preliminary experiments and considerations. In general, the absorption of light in a solid is completed within 20-100 nm ($200\text{-}1000 \text{ \AA}$) of light path, which is close to the light skin depth of the material with the exception of highly absorptive materials like carbon black. Carbon black is difficult to prepare and hard to handle as a thin film. Vacuum deposition of thin metal films is quite easy to obtain but is highly reflective at low light energy levels. However, at high light energy levels, a plasma is formed which increases the absorptivity by orders of magnitude. Aluminum was selected because it has a low melting point and is easy to vacuum deposit on a glass substrate. Other metals may be more efficient, but a study to optimize the target material was not made.

The optimum thickness of the target material was found to be about 100 nm (1000 \AA). Films thicker than 100 nm caused the average dynamic transmission of the Q-switched laser light to be less than 1.0%, and the amount of post-irradiated film remaining became significant (Fig.

¹ Values in customary units are included in parentheses after values in SI (International System) units if the customary units were used in the measurements or calculations.

3). There would be no advantage in increasing the thickness, because the additional mass would result in a lower temperature and pressure in the plasma during the laser absorption period. Films thinner than 100 nm were completely vaporized before absorption of all the laser energy. Aluminum targets of various thickness were irradiated with 1.67 J of focused laser energy; the shocks generated are shown in Fig. 4.

III. Test Apparatus

A Korad K-1Q laser system with a KDP Pockel cell^{*} was capable of producing 4.5 J of energy in a pulse width of 25 ns. The laser head utilized a ruby rod 1.43 cm in diameter and 7.6 cm long. The laser beam was focused with a double convex lens 30 cm in focal length. An extra 6-plate Brewster stack polarizer was used to completely eliminate prelasering at high pumping levels.

A schematic of the experimental configuration is shown in Fig. 5. A Beckman-Whitley Model 200 Simultaneous Streak and Framing Camera was used to record the event. The steel mirror was operated at 1000 rev/s, which corresponds to a writing speed of $2.76 \text{ mm}/\mu\text{s}$, or at a time resolution of 50 ns. The laser power supply was triggered by a synchronous sequence when the rotating mirror reached a preset position and speed.

The laboratory arrangement for conducting the experiments is shown in Fig. 6. The explosive sample is placed in a safety chamber and aligned with the laser. The laser pulse enters the chamber through a portal containing the focusing lens. The streak camera is aligned perpendicular to the axis of the explosive column. Several different explosive test vehicles were used, which contained viewing optics so that the light from the reaction could be recorded.

Figure 7 shows a test vehicle in which a plastic rod serves as the viewing port. The glass window with the metal film facing the explosive column is held in the cavity provided with an end plate to contain it. The explosive under test is then loaded against the window. A cold-rolled steel witness block completes the test vehicle assembly.

A second test vehicle is shown in Fig. 8. The explosive is loaded into a glass tube and then assembled into a brass fixture in much the same manner as the previous assembly. The components are interference-fitted because good confinement is critical in the initial phase of ignition.

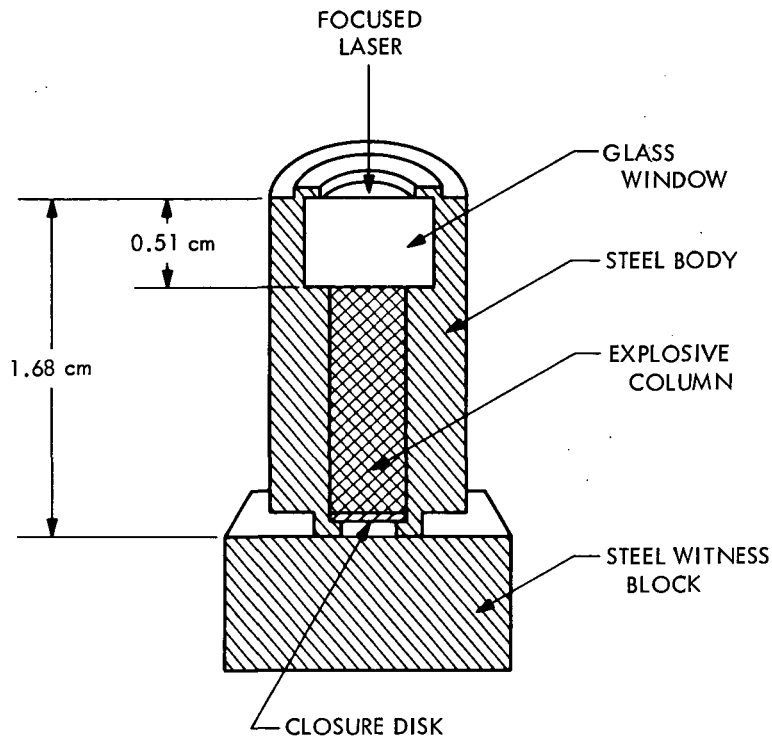


Fig. 1. Test vehicle for laser initiation study

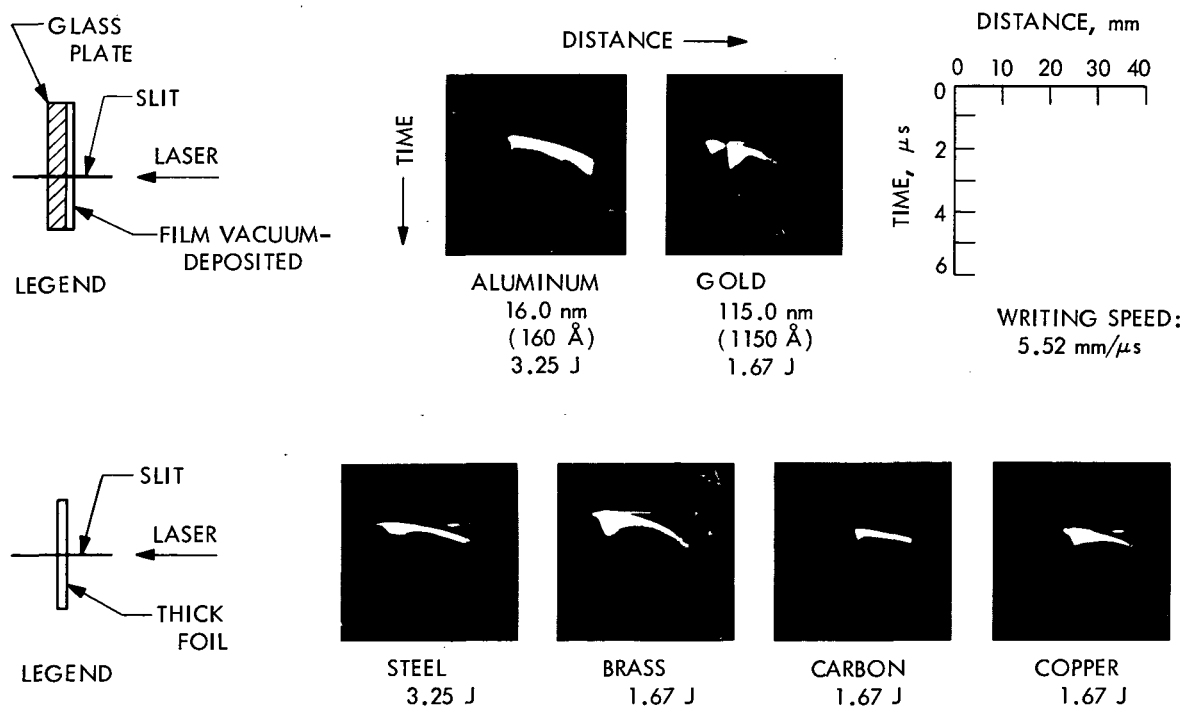
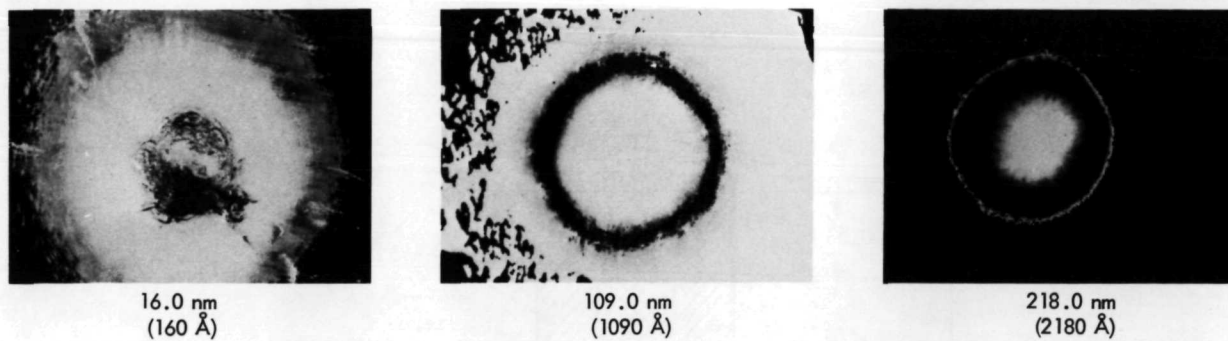


Fig. 2. Streak camera records of the plasma generated in a vacuum from a focused Q-switched ruby laser



ALUMINUM FILMS VACUUM-DEPOSITED ON A GLASS SUBSTRATE
 MAGNIFICATION X 14.5
 LASER ENERGY = 2.5 J
 FOCAL LENGTH OF LENS = 30 cm

Fig. 3. Post-irradiation damage to thin aluminum films by a focused Q-switched ruby laser

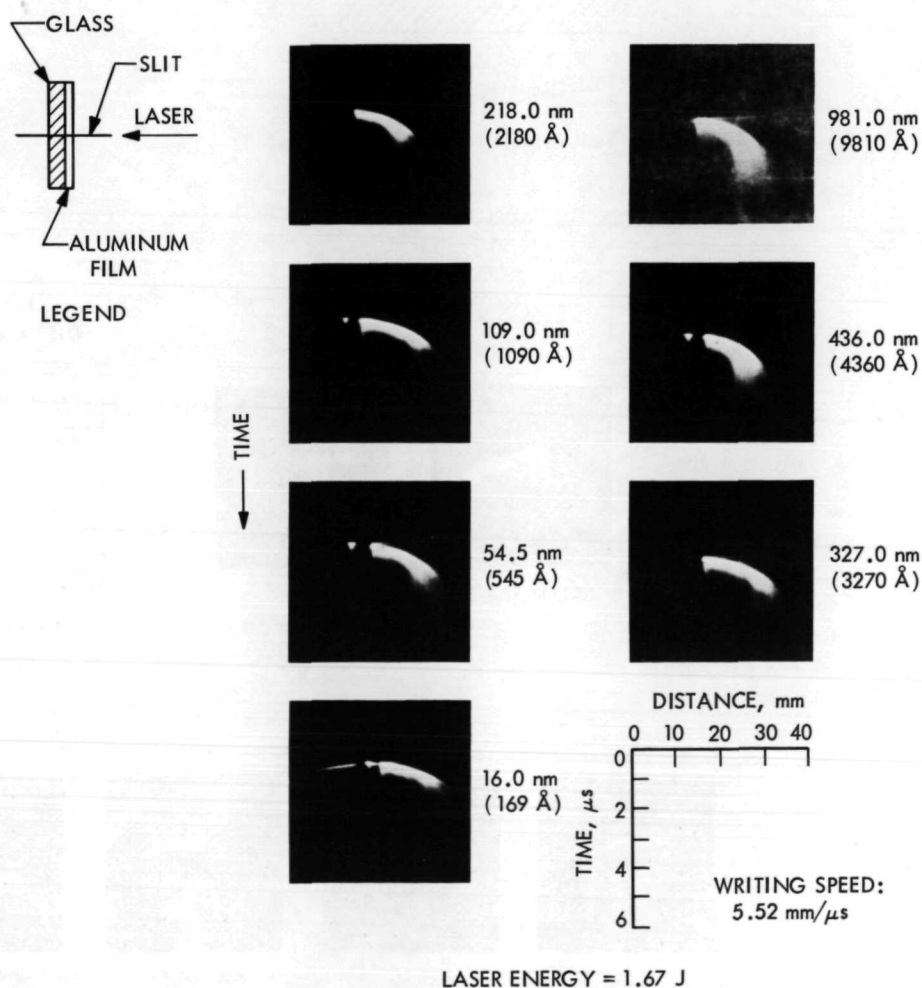


Fig. 4. Streak camera records of the plasma generated in a vacuum, for various thicknesses of aluminum films, from a focused Q-switched ruby laser

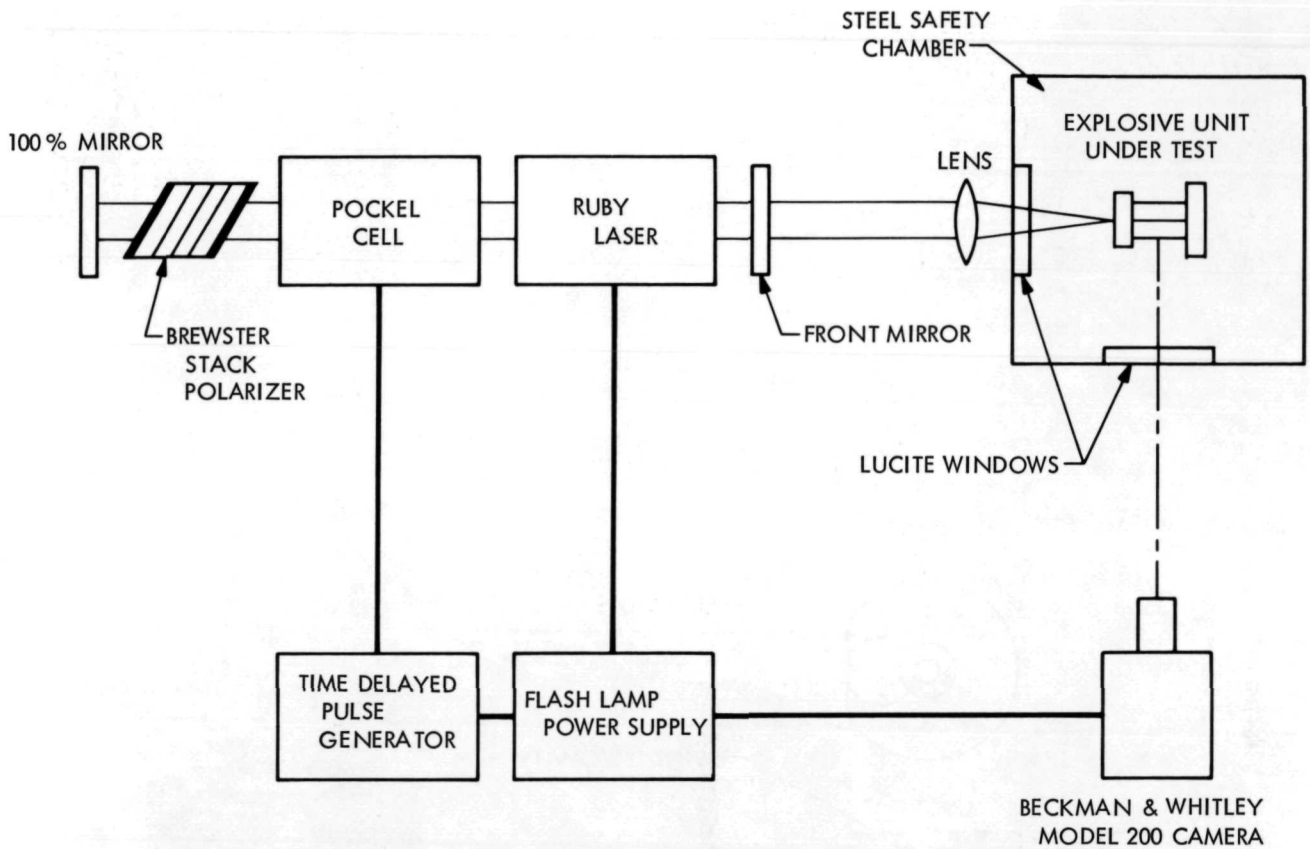


Fig. 5. Block diagram of experimental configuration

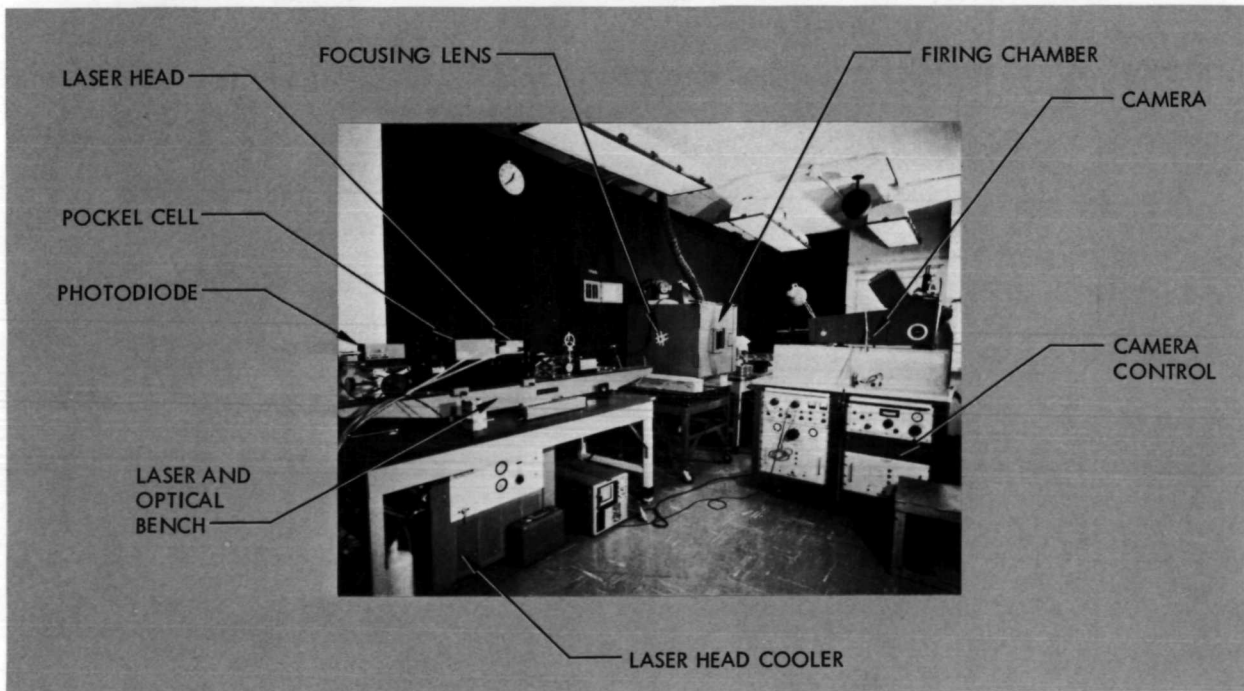


Fig. 6. Laboratory arrangement of laser, camera, and firing chamber

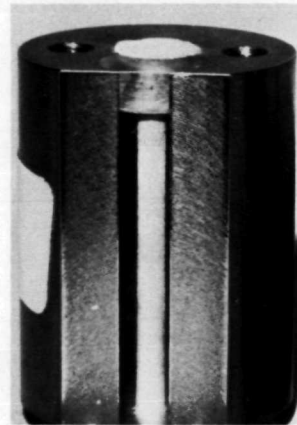
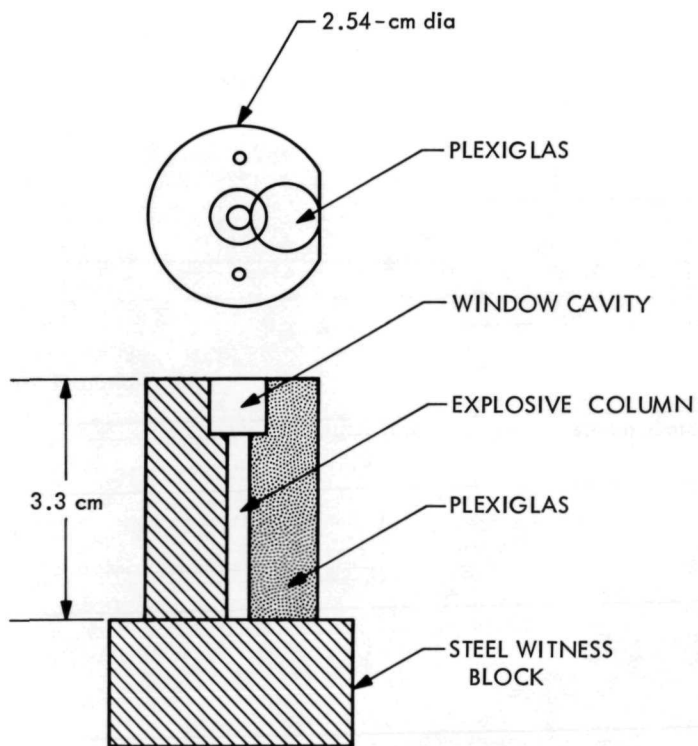


Fig. 7. Test vehicle with plastic viewing window for laser initiation study

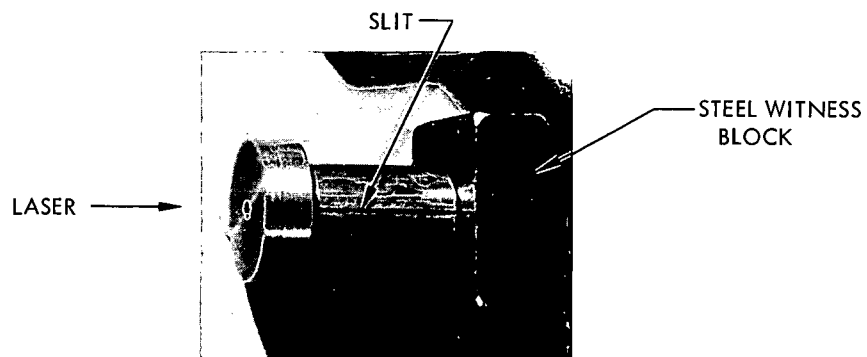
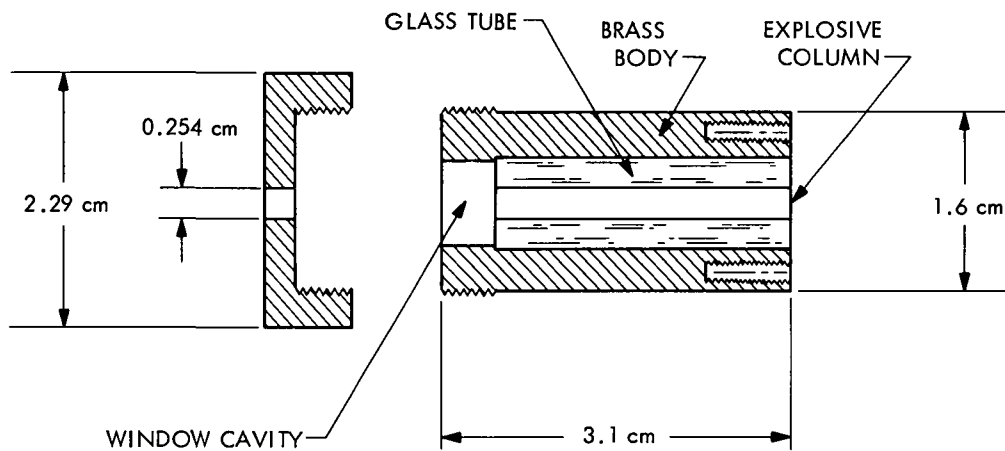


Fig. 8. Test vehicle with glass tube configuration for viewing of laser initiation

IV. Test Results

Approximately 90 firings were made involving five different explosives: PETN, RDX, tetryl, hexanitro stilbene (HNS), and Dipam. The different parameters studied were density, particle size, explosive diameter, laser energy, and the use of plain or aluminized windows. Dipam and HNS did not detonate under any of the conditions tested, although in two cases HNS completely burned at maximum energy input. Table 1 summarizes the results.

As expected, PETN was the most sensitive to laser energy of the explosives tested. The minimum energy required was below 1.0 J at $34.5 \times 10^6 \text{ N/m}^2$ (5 kpsi) loading pressure.¹ Detonations were observed with 2 J of laser energy at loading pressures up to $172.5 \times 10^6 \text{ N/m}^2$ (25 kpsi). The PETN particle size did not appear to be critical to laser detonation. Table 2 summarizes the PETN data.

The RDX was tested at loading pressures ranging from 6.89×10^6 to $345 \times 10^6 \text{ N/m}^2$ (1 to 50 kpsi). Ignitions were observed up to $345 \times 10^6 \text{ N/m}^2$ but immediate detonation occurred only up to $34.5 \times 10^6 \text{ N/m}^2$. Particle size apparently influenced the detonability of RDX, since no detonations were observed with coarse material. (This observa-

¹ Values in customary units are included in parentheses after values in SI (International System) units if the customary units were used in the measurements or calculations.

tion agrees with Stresau's results in Ref. 9). Most detonations occurred when an aluminized window was used. The RDX results are summarized in Table 3.

Only seven tests have been completed with tetryl. Two detonations were observed with milled tetryl at $6.89 \times 10^6 \text{ N/m}^2$ (1 kpsi) loading pressure and aluminized windows. Under the same conditions, but using a plain window, detonation did not occur. The results from these tests are summarized in Table 4.

The streak camera records of most of the items that detonated were analyzed for total reaction time (time from laser pulse to the end of the reaction), transient time (time from laser pulse to start of steady-state detonation), and steady-state detonation velocity. Several items that detonated are omitted because of the poor quality of the streak record. Table 5 summarizes the data and compares the measured detonation velocities with ideal detonation velocities. The measured detonation velocities are close to the ideal detonation velocities. Steel dent values are also listed, and the depth values are directly ordered with the detonation velocity.

Figures 9, 10, and 11 show some of the smear records obtained of the items in Table 5. In the case of PETN, where coarse powder was used, the transient time is quite long (microseconds) when compared to the tenths of microseconds for milled PETN. One RDX test had a zero

Table 1. Conditions and results for laser testing of HNS and Dipam

Test	Explosive	Particle size	Loading pressure		Laser energy, J	Charge diameter, cm	Charge length, cm	Confinement	Window	Results
			10^6 N/m^2	kpsi						
1	HNS	M	6.90	1	4.0	0.3	2.54	Glass	P	Failed to ignite
2		M	6.90	1	4.0	0.3		Glass	Al	Failed to ignite
3		C	6.90	1	4.2	0.24		Steel		Failed to ignite
4			34.5	5	4.2	0.24		Steel		Burned completely
5			69.0	10	4.2	0.24		Steel		Burned completely
6					3.0	0.3	2.54	Glass		Failed to ignite
7					3.0	0.3	2.03	Glass		
8			69.0	10	3.0	0.3	2.03	Glass		
9	HNS	C	345	50	4.2	0.24	2.54	Steel		
10	Dipam	M	6.90	1	3.8	0.27	2.03	Steel	Al	
11	Dipam	M	6.90	1	3.8	0.27	2.03	Steel	P	
12	Dipam	C	69.0	10	3.0	0.3	2.54	Glass	Al	

M = Milled for 16 h in chloroform.

C = Coarse (as received).

P = Plain glass window.

Al = 100-nm (1000-Å) aluminized glass window in contact with explosive.

transient time. Tetryl had a relatively long transient time of 1.45 μs . It is noted that the laser energy listed is the energy measured at the laser head. The lens, lucite entrance window, and glass window each transmit about 92% of light energy.

V. Discussion

In some instances in the tables, a burn to detonation is recorded rather than a detonation or complete burn. The streak camera results for these cases showed burning during the writing time of the camera. Later the reaction went to detonation, which was verified by a dent in the steel witness block. All the streak camera records showed light streaks at the fixture surface/air interface and along the length of the explosive column. This light was emitted when the margin of the laser focal spot interacted with the metal surface. The laser light was also scattered diffusively through the glass tubing or lucite rod.

It is apparent that for PETN and RDX, instantaneous detonations were achieved. In some cases, the transient times were less than 0.5 μs , and variations in detonation velocity were less than 10%. The PETN did not exhibit an increase in sensitivity when the aluminized window

was substituted for the plain window. The initiation mechanism for PETN may be very complicated, so that the effects of the aluminized window are overshadowed by other mechanisms. The RDX appears to be more sensitive to detonation when the aluminized window is used. Tetryl definitely demonstrated that the aluminized window is necessary to achieve detonation. In all cases, the fine particle size (less than 40 μs) and loading pressures below $34.5 \times 10^6 \text{ N/m}^2$ (5 kpsi) increased the explosive sensitivity.

Comparison of the laser detonation results with EBW studies shows that laser-induced detonations are not as sensitive to loading density as are detonations with EBW. This may be due to the much higher shock velocity generated by the laser. Probably for this same reason, explosives less sensitive than PETN were directly detonated. Small deviations from 1.0 g/cm^3 in EBW applications make a considerable difference in sensitivity. Because explosives loaded at densities greater than 1.0 g/cm^3 can be laser-detonated, a correspondingly higher detonation velocity can be achieved. The detonation velocities obtained by laser initiation are closer to the ideal detonation velocity than those reported by EBW initiation.

Table 2. Conditions and results for laser testing of PETN

Test	Particle size	Loading pressure		Laser energy, J	Charge diameter, cm	Charge length, cm	Confinement	Window	Results
		10^6 N/m^2	kpsi						
1	M	34.5	5	0.8	0.38	2.06	Steel	P	Detonated
2	M	34.5	5	0.5	0.38	2.06	Steel	Al	Burn to detonation
3	M	34.5	5	0.8	0.38	2.79	Steel		Detonated
4	C	69.0	10	4.0	0.3	2.03	Glass		Burned
5				4.0		2.03			Detonated
6				3.0		2.03			Detonated
7						2.54			Failed to ignite
8					0.3	2.54	Glass	Al	Detonated
9	C			3.0	0.38	2.79	Steel	P	
10	M			1.0		2.06		P	
11		69.0	10	1.0				Al	Detonated
12		172.5	25	0.8				P	Burned
13				0.8				Al	Burned
14				2.0				P	Detonated
15				2.0	0.38	2.06	Steel	Al	Burned
16				3.4	0.3	2.54	Glass	Al	Failed to ignite

M = Milled for 16 h in chloroform.

C = Coarse (as received).

P = Plain glass window.

Al = 100-nm (1000-Å) aluminized glass window in contact with explosive.

Table 3. Conditions and results for laser testing of RDX

Test	Particle Size	Loading pressure		Laser energy, J	Charge diameter, cm	Charge length, cm	Confinement	Window	Results
		10^6 N/m^2	kpsi						
1	M	6.90	1	1.0	0.3	2.54	Glass	P	Detonated
2				1.0	0.3	2.54	Glass	Al	Detonated
3				1.5	0.1	2.54	Glass		Detonated
4				3.5	0.27	2.06	Steel		Burn to detonation
5				3.5	0.1	2.54	Glass		Detonated
6				3.8	0.27	2.06	Steel	Al	Detonated
7	M			3.8	0.27	2.06		P	Burn to detonation
8	C			3.5	0.38	2.79		Al	Complete burn
9	M			4.0	0.1	1.78			Detonated
10	C	6.90	1	4.2	0.38	1.01	Steel		Failed to ignite
11	M	34.5	5	1.0	0.3	2.54	Glass	Al	
12				1.0	0.3			P	
13				2.85	0.3			P	Failed to ignite
14				3.13	0.3			Al	Detonated
15				3.5	0.1	2.54	Glass		Detonated
16				3.5	0.27	2.06	Steel		Failed to ignite
17				3.8	0.27	2.06		Al	Detonated
18				3.8	0.27	2.06		P	Detonated
19	M			4.0	0.1	1.78		Al	Detonated
20	C	34.5	5	4.2	0.38	1.01		Al	Complete burn
21	C	69.0	10	1.0	0.38	2.79	Steel	Al	Failed to ignite
22	M			2.1	0.3	2.54	Glass	P	Failed to ignite
23	M			2.1		2.54		Al	Failed to ignite
24	C			3.0		2.03			Complete burn
25						2.54			Failed to ignite
26						2.54			Failed to ignite
27					0.3	2.54	Glass		Failed to ignite
28					0.51	0.76	Steel		Complete burn
29					0.38	2.79		Al	Complete burn
30					0.38	2.79		P	Complete burn
31					0.38	2.79		Al	Failed to ignite
32				3.0	0.24	2.54			Burn to detonation
33				3.5	0.24				Complete burn
34	C			3.5	0.24		Steel	Al	Complete burn
35	M			3.8	0.3	2.54	Glass	P	Failed to ignite
36	C			4.0	0.38	2.79	Steel	Al	Complete burn
37	C				0.38	2.79			Complete burn
38	M				0.1	1.78			Failed to ignite

M = Milled for 16 h in chloroform.

C = Coarse (as received).

P = Plain glass window.

Al = 100-nm (1000-Å) aluminized glass window in contact with explosives.

Table 3. (contd)

Test	Particle Size	Loading pressure		Laser energy, J	Charge diameter, cm	Charge length, cm	Confinement	Window	Results
		10^6 N/m ²	kpsi						
39	M				0.27	2.06	Steel		Complete burn
40	M			4.0	0.3	2.54	Glass		Failed to ignite
41	C			4.2	0.38	2.79	Steel		Complete burn
42				4.3	0.24	2.54			Complete burn
43				4.3	0.27	2.06			Complete burn
44				4.2	0.38	1.01			Complete burn
45	C			4.2	0.27	2.06	Steel		Complete burn
46	M			4.4	0.3	2.54	Glass	Al	Failed to ignite
47	M	69.0	10	4.6	0.3	2.54	Glass	P	Failed to ignite
48	C	207	30	4.0	0.38	2.79	Steel	P	Complete burn
49		207	30	4.0	0.38	2.79		Al	Failed to ignite
50		207	30	4.0	0.23	2.79			Complete burn
51		345	50	4.2	0.38	1.01			Failed to ignite
52		345	50	4.2	0.38	1.01			Complete burn

Table 4. Conditions and results for laser testing of tetryl

Test	Particle size	Loading pressure,		Laser energy, J	Charge diameter, cm	Charge length, cm	Confinement	Window	Results
		10^6 N/m ²	kpsi						
1	M	6.90	1	3.8	0.27	2.06	Steel	Al	Burn to detonation
2				3.8	0.38	2.06	Steel	P	Complete burn
3				4.0	0.3	2.54	Glass	P	Fail to initiate
4	M	6.90	1	4.0	0.3	2.54	Glass	Al	Detonated
5	C	69.0	10	3.0	0.3	2.03	Glass		Fail to initiate
6	C	69.0	10	3.0	0.38	2.54	Steel		Fail to initiate
7	C	138	20	3.0	0.51	0.76	Steel		Complete burn

M = Milled for 16 h in chloroform.

C = Coarse (as received).

P = Plain glass window.

Al = 100-nm (1000-Å) aluminized glass window in contact with explosive.

Table 5. Conditions and results for selected laser-detonated items

Test	Explosive	Particle size	Density, g/cm ³	Laser energy, J	Charge diameter, cm	Charge column length, cm	Confinement	Window	Time, μ s		Detonation velocity, mm/ μ s		Steel dent depth, mm
									Total	Transient	Measured	Ideal ^a	
1	PETN	M	1.58	0.8	0.38	2.06	Steel	P	3.11	0.54	7.011	7.841	0.64
2			1.58	0.8		2.79		Al	4.82	0.72	7.724	7.841	0.59
3			1.64	1.0		2.06		P	2.97	0.80	7.620	8.078	0.76
4		M		1.0	0.38	2.06	Steel	Al	2.90	0.43	7.228		0.61
5		C		3.0	0.30	2.06	Glass	Al	4.05	1.98	7.346		0.53
6				3.0	0.30	2.54	Glass	Al	6.95	3.96	5.601		0.22
7				3.0	0.38	2.79	Steel	P	6.48	2.90	6.836		0.81
8		C	1.64	4.0	0.30	2.03	Glass	Al	9.42	6.68	5.604	8.078	0.18
9	PETN	M	1.72	2.0	0.38	2.06	Steel	P	2.86	0.36	7.379	8.394	0.76
10	RDX		1.18	1.0	0.30	2.54	Glass	P	5.43	1.66	6.491	6.728	0.46
11				1.0	0.30			Al	3.98	0.00	6.374		0.38
12				1.5	0.10				7.17	2.53	5.476		0.20
13				3.5	0.10	2.54	Glass		5.00	0.30	5.393		0.13
14			1.18	3.8	0.27	2.06	Steel		4.16	0.60	5.750	6.728	0.46
15			1.52	2.85	0.30	2.54	Glass		4.17	0.76	6.741	7.946	0.53
16				3.5	0.10	2.54	Glass		5.30	0.40	5.608		0.28
17				3.8	0.27	2.06	Steel	Al	3.62	0.72	6.741		0.53
18	RDX		1.52	3.8	0.27	2.06	Steel	P	3.73	0.54	5.992	7.946	0.58
19	TETRYL		1.08	4.0	0.30	2.54	Glass	Al	5.43	1.45	5.609	5.858	0.23

M = Milled for 16 h in chloroform.

P = Plain glass window.

C = Coarse (as received).

Al = 100-nm (1000-Å) aluminized glass window in contact with explosive.

^aM. A. Cook, *The Science of High Explosives*, Reinhold Publishing Corp., N.Y., 1958.

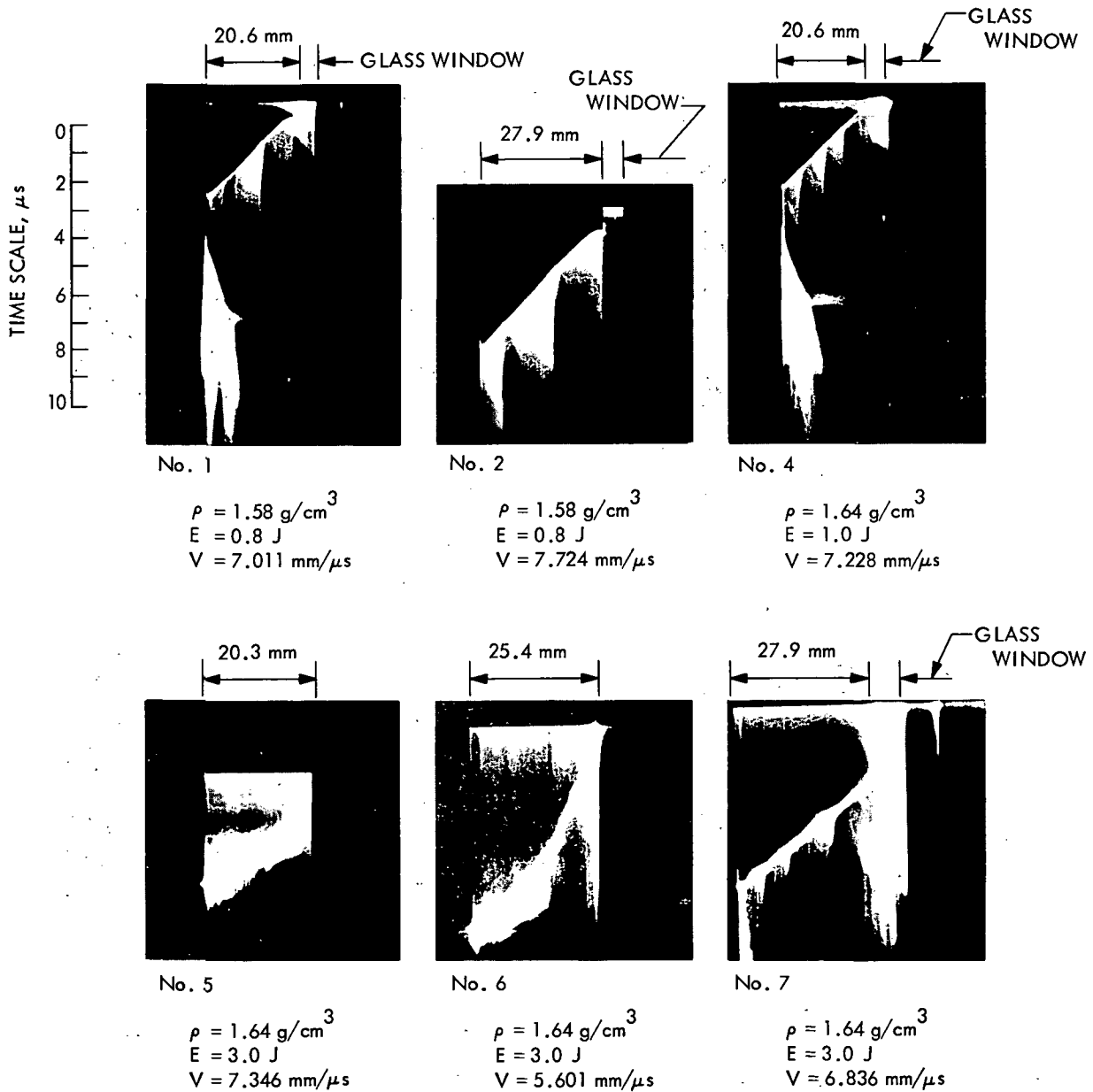


Fig. 9. Streak camera records of laser-initiated detonation in PETN (values given refer to Table 5)

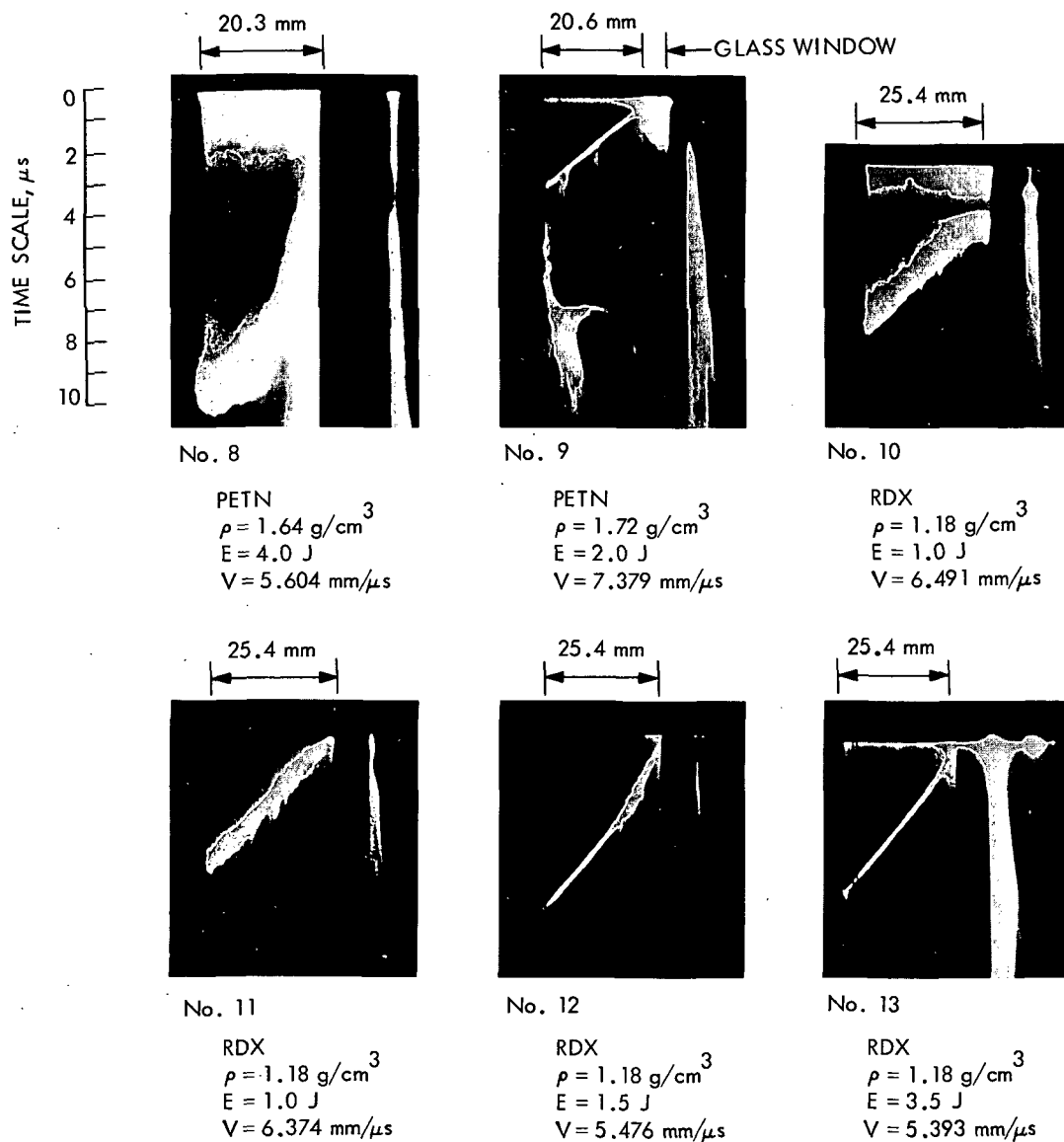


Fig. 10. Streak camera records of laser-initiated detonation in PETN and RDX (values given refer to Table 5)

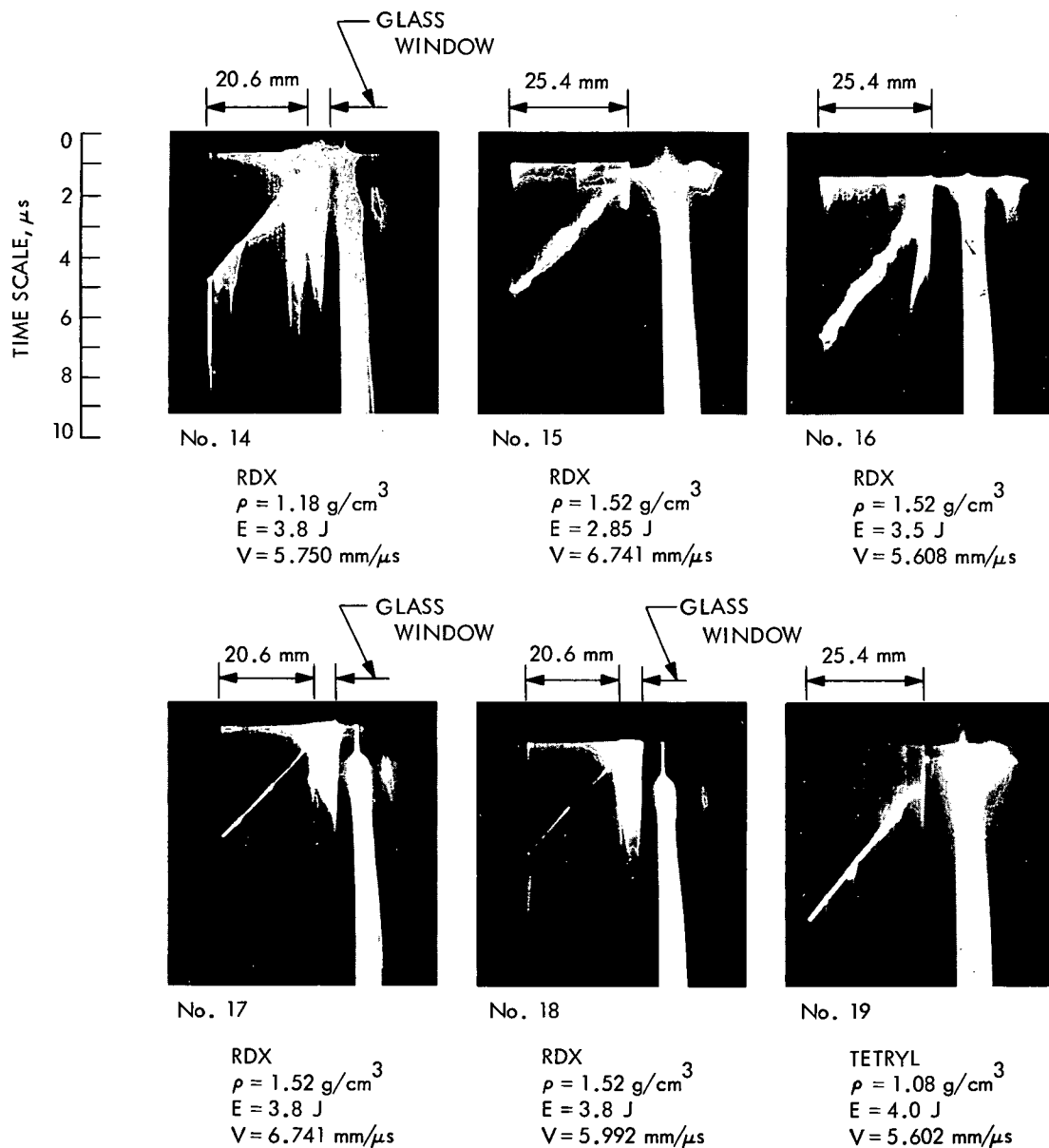


Fig. 11. Streak camera records of laser-initiated detonation in RDX and tetryl (values given refer to Table 5)

References

1. Bowden, F.P., and Yoffe, A.D., *Fast Reactions in Solids*, Butterworth's Scientific Publications, 1958.
2. Leopold, H.S., Initiation of Explosives by Exploding Wires III, *NOLTR 64-2*. U.S. Naval Ordnance Laboratory, White Oak, Silver Spring, Maryland, Mar. 17, 1964.
3. Scott, C.L., "Effect of Particle Size on Shock Initiation of PETN, RDX, and Tetryl," *Fifth Symposium on Detonation*, U.S. Naval Ordnance Laboratory, White Oak, Silver Spring, Maryland, Aug. 1970.
4. Menichelli, V.J., and Yang, L.C., *Sensitivity of Explosives to Laser Energy*, Technical Report 32-1474. Jet Propulsion Laboratory, Pasadena, California, Apr. 30, 1970.
5. Barbarisi, M.J., and Kessler, E.G., *Initiation of Secondary Explosives by Means of Laser Radiation*, Technical Report 3861. Picatinny Arsenal, Dover, New Jersey, May 1969.
6. Brish, A.A., et al., "Initiation of Detonations in Condensed Explosives with a Laser," *Combust. Explosive Phys.*, No. 3, 1966, pp. 132-133.
7. Yang, L.C., and Menichelli, J., "Detonation of Insensitive High Explosives by a Q-Switched Ruby Laser," *Appl. Phys. Lett.*, Vol. 19, No. 11, Dec. 1, 1971.
8. Basov, N.G., et al., Letter 6, *JETP*, p.168, Sept. 15, 1967.
9. Stresau, R.H.F., et al., "Confinement Effects in Exploding Bridgewire Initiation of Detonation," *Fourth Symposium on Detonation*, U.S. Naval Ordnance Laboratory, White Oak, Silver Spring, Maryland, Oct. 1965